电流模式变换器的建模、分析和补偿

概述

随着电流变换技术的流行，固定频率、峰值电流检测控制方案的几个特点显现了出来。包括占空比大于 50%时不稳定、次谐波振荡的倾向、响应不够理想、对噪声敏感。本文试图说明，对于任何电流模式变换器，如果对电流波形的采样附加固定量的斜坡补偿，可以减轻或消除上述所有问题，同时从而使变换器的性能得到提升。

1.0 简介

近来在电流控制模式中，引进了完整的控制电路并大量应用于新的设计。尽管已经充分证明了电流模式控制方式比传统的电压控制方式有优势，但是对于固定频率峰值电流控制模式的变换器，依然存在一些缺点。它们是：(1) 占空比大于 50%时的开环不稳定性；(2) 电感峰值电流代替平均电流导致的响应不理想；(3) 次谐波振荡的倾向；(4) 特别是电感的纹波电流较小时对噪声敏感。尽管在大多数场合，电流控制模式的好处远远超过这些缺点，还是需要简单可行的解决方案的。很多论述表明，在电流波形上添加斜坡补偿可以使系统在占空比超过 50%时保持稳定（图 1）。

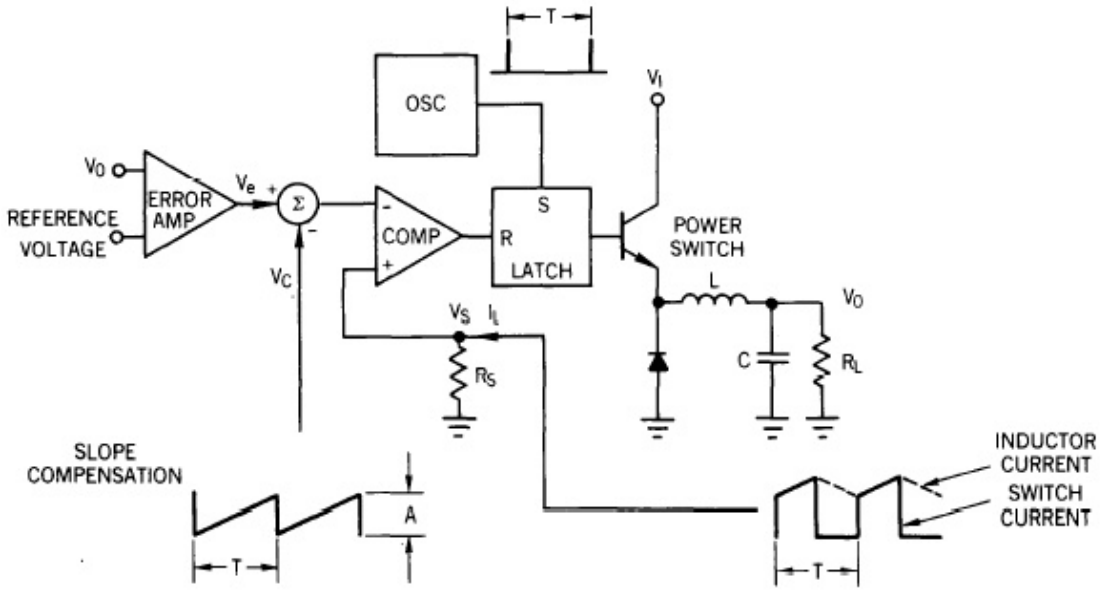

FIGURE 1 - A CURRENT-MODE CONTROLLED BUCK REGULATOR WITH SLOPE COMPENSATION.

另外，同样的补偿技术也能够用来改善上述的几乎所有缺点。实际上，在实用的变换器中对电流波形采用斜坡补偿几乎总能使性能提升。

简单的添加斜坡补偿，通常用一个电阻，这种做法很有吸引力。然而，这带来了一个新问题，即如何分析和预测变换器的性能。文献中已经大量研究了电流和电压模式的 PWM 小信号交流模型。斜坡补偿或“双环控制”的变换器各自采用不同的元器件构成电路，但他们拥有共同的特性。尽管已经有多位作者指出了这点，仍然有必要给电源设计者提供一个能够定性和定量的简单电路模型。

这篇论文的首要目的是让读者熟悉峰值电流控制变换器的特点，并同时论证了斜坡补偿技术削弱或消除问题的能力。这些内容第 2 部分。第二，在第 3 部分采用（1）描述的状态空间平均技术研究了的连续电流模式斜坡补偿 BUCK 变换器电路模型。这给在第 4 部分讨论实际采用斜坡补偿提供了分析的基本原理。

2.1 开环不稳定性

不管电压反馈环的状态，对任何固定频率电流模式，当占空比超过 50%**时，在内环电流环存在固有的不稳定性。虽然一些拓扑（最著名的如双管正激变换器），占空比不能超过** 50%**，然而其他的更多拓扑则要求更大的占空比，否则输入将受到严重的限制。通过在内环引入少量的斜坡补偿，可以在所有的占空比范围实现稳定性。下面简单地回顾一下这项技术。**

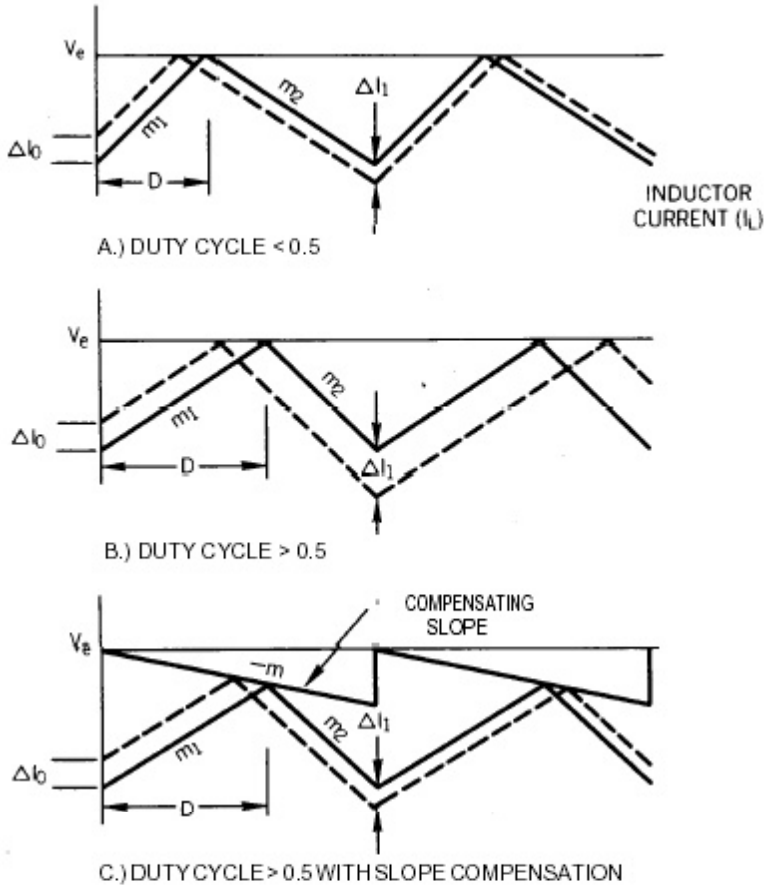

FIGURE 2 - DEMONSTRATION OF OPEN LOOP INSTABILITY IN A CURRENT-MODE CONVERTER.

图 2 **描述了一个电流模式变换器的电感电流** I_L **受误差电压** V_e **控制的波形。通过图形可以看出，给电流** I_L **一个扰动量△I，当** D<0.5 **时，扰动将会减小（图** 2A**），而当** D>0.5 **时，扰动将会增加（图** 2B**）。用数学式表示为：**

$$\Delta I_1 = -\Delta I_O\left(\frac{m_2}{m_1}\right) \qquad (1)$$

更进一步，我们可以引入象图 2C **那样的一个线性的斜坡-**m**。注意这个斜坡可以加在电流波形上，或从误差电压减去。于是，我们得到：**

$$\Delta I_1 = -\Delta I_O\left(\frac{m_2 + m}{m_1 + m}\right) \qquad (2)$$

可以算出，当

$$m > -\frac{1}{2}m_2 \qquad (3)$$

时，系统稳定。所以，为了保证电流环的稳定，补偿的斜率必须大于电流波形下降斜率的一半。对于图 1 **所示的** BUCK **变换器，**m_2 **是一个常数，等于**(Vo/L)*Rs**。因此，补偿的幅度应该为**

$$A > TR_s\frac{V_O}{L} \qquad (4)$$

以保证占空比大于 50%时的稳定性。

2.2 电感电流振荡

仔细观察电感电流波形，可以发现与先前不稳定性相关的两种其他现象。如果我们推广等式 2 并在图 3 中画出 nT 周期内每个的 In，我们可以观察到频率为开关频率一半的象一个 RLC 电路一样的阻尼正弦波。这个振铃输出是不好的。(a) 它会使电感电流产生振荡影响输入和负载的瞬态响应。(b) 使闭环增益的峰值出现在 1/2 的开关频率处，引入了显著的不稳定倾向。

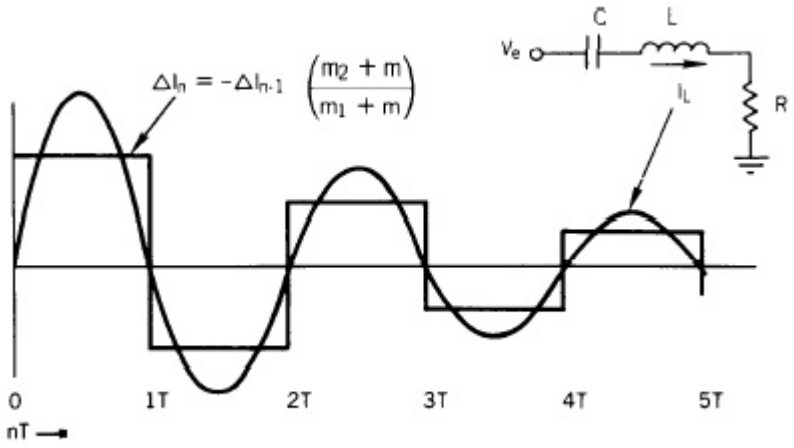

FIGURE 3 - ANALOGY OF THE INDUCTOR CURRENT RESPONSE TO THAT OF AN RLC CIRCUIT.

就象在（1）中所说的，也很容易从等式 2 验证，如果选择补偿的斜率 m 等于$-m_2$（电感电流下降斜率），可以得到最好的瞬态响应。这于 RLC 临界阻尼电路相似，允许电流在一个周期校正自身。图 4 用图形证明了这一点。

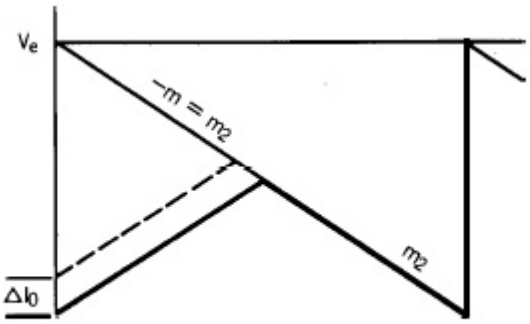

FIGURE 4 - FOR THE CASE OF m = - m_2, A CURRENT PERTURBATION WILL DAMP OUT IN EXACTLY ONE CYCLE.

注意这可能是最好的电感电流振荡波形，基本于电压控制环本身的瞬态响应无关。

2.3 次谐波振荡

电流内环的增益峰值是一个和电流模式控制器相关的最重要的问题之一。这个峰值产生在开关频率的一半处，并会因为调整器的过度相移，而导致电压反馈环进入在频率为一半开关频率的振荡。这种不稳定性，有时称为次谐波振荡，非常容易使功率传输过程中，连续的两个驱动脉冲的占空比不对称。 图 5 显示了一个电流模式控制器的电感电流处于次谐波振荡的现象（显示了两个周期）。

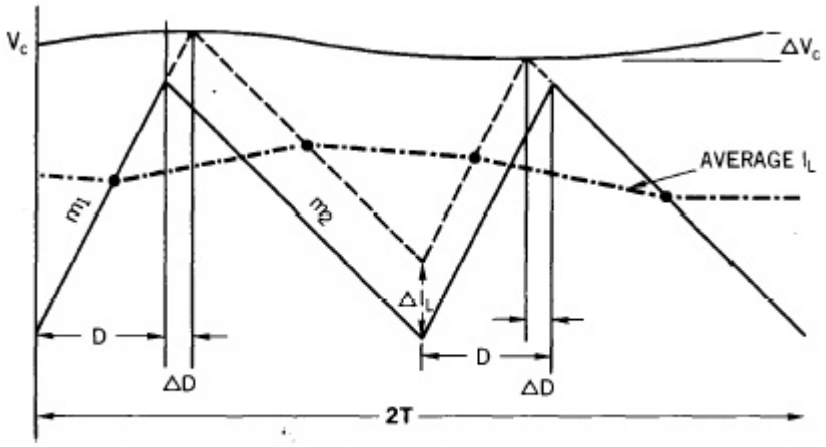

FIGURE 5- CURRENT WAVE FORM (DOTTED) OF A CURRENT-MODE CONVERTER IN SUBHARMONIC OSCILLATION.

为了确定稳定的范围，有必要发展一个内环在一半开关频率处的增益表达式。在（2）里的技术相当于包括附加了斜坡补偿 BUCK 变换器。

2.3.1 在 1/2 fs 处开环的增益计算

参考图 5 和图 6，我们希望建立输入信号$\triangle V_O$和输出电流$\triangle I_L$的关系。根据图 5，两个等式可以写为：

$$\triangle I_L=\triangle Dm_1T-\triangle Dm_2T \qquad (4)$$

$$\triangle V_C=\triangle Dm_1T+\triangle Dm_2T \qquad (5)$$

如图 6 那样增加了斜坡补偿后，给出另一个等式

$$\triangle V_e=\triangle V_C+2\triangle DmT \qquad (6)$$

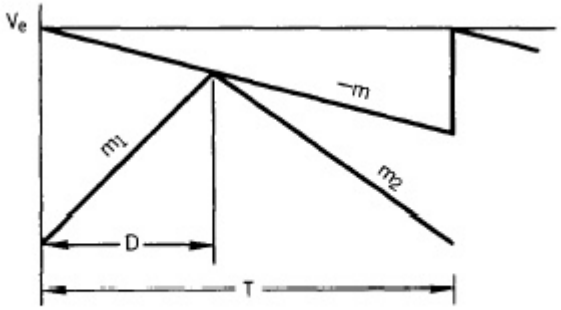

FIGURE 6- ADDITION OF SLOPE COMPENSATION TO THE CONTROL SIGNAL

用（5）消去（6）中的$\triangle V_C$，得到$\triangle I_L/\triangle V_e$的表达式：

$$\frac{\Delta I_L}{\Delta V_e}=\frac{m_1-m_2}{m_1+m_2+2m} \qquad (7)$$

对于稳定状态的条件可以写为：

$$Dm_1T=-(1-D)m_2T \qquad (8)$$

或

$$D=\frac{-m_2}{m_1-m_2}$$

用（9）式将（7）式简化，得到

$$\frac{\Delta I_L}{\Delta V_e}=\frac{1}{1-2D(1+m/m_2)} \qquad (10)$$

现在，通过确认$\triangle I_L$在 2T 的周期内，是简单的方波波形。我们可以用因子 $4/\pi$算出$\triangle I_L$的一次谐波的幅值并写出在 $f=1/2f_S$ 处的小信号增益：

$$\frac{i_L}{v_e}=\frac{4/\pi}{1-2D\ (1+m/m_2)} \qquad (11)$$

如果我们假定一个容性的输出负载为 C，误差放大器的增益为 A，在 $f=1/2f_s$ 的开环增益表达式最终为：

$$\text{开环增益}=\frac{\frac{4TA}{\pi^2C}}{1-2D\ (1+m/m_2)} \qquad (12)$$

2.3.2 用斜坡补偿消除次谐波振荡

从等式 12，我们能写出在 $f=1/2f_s$ 处，能保证稳定的误差放大器的最大增益的等式为：

$$A_{max}=\frac{1-2D\ (1+m/m_2)}{\frac{4T}{\pi^2C}} \qquad (13)$$

这个等式清楚地说明，误差放大器最大允许的增益是占空比和斜坡补偿的函数。一个 A_{max} 与数个斜坡补偿相对与占空比的规格化图显示在图 7。

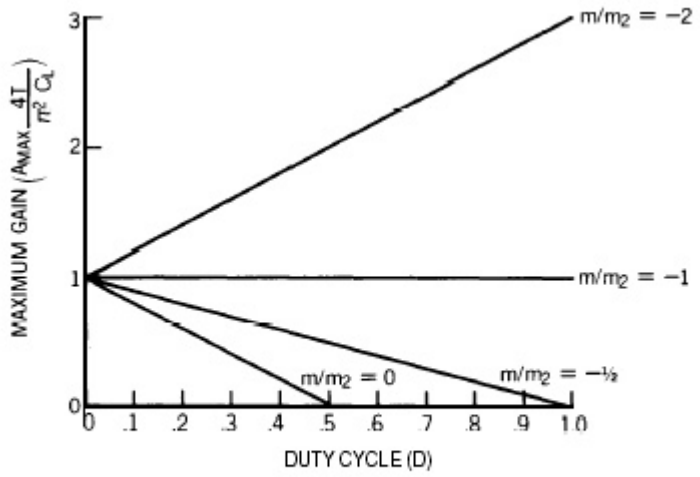

FIGURE 7 - MAXIMUM ERROR AMPLIFIER GAIN AT ½f_s (NORMALIZED) V.S. DUTY CYCLE FOR VARYING AMOUNTS OF SLOPE COMPENSATION. REFER TO EQUATION 13.

假设误差放大器的增益在 $f=1/2f_s$ 处不能降到零，对于 m=0（不补偿）的情形，可以看到象先前讨论的那样，在 50%的占空比处不稳定。当将补偿增加到 $m=-1/2m_2$，不稳定的点移动到了占空比为 1 处。然而，在任意的实际系统中，有限的 A_{max} 将导致反馈环在达到最大占空比之前就进入次谐波振荡。如果我们继续增加 m，达到 $m=-m_2$ 这个点，最大增益变的和占空比无关了。这个点就是象先前讨论的，是临界阻尼点。增加 m 的值超过这个点，将对整个占空比范围内提高调整器的稳定性基本没有帮助。

2.4 峰值电流检测与平均电流检测的对比

真实的电流模式变换，根据定义，平均电感电流应该跟随误差电压变化。实际上用电流源代替电感并简化系统。然而如图 8 所示，通常使用的峰值电流检测允许平均电感电流随占空比变化，产生不完美的输入输出或前馈特性。如果我们选择添加 $m=-1/2m_2$ 斜坡补偿，如图 9，我们就能够转换峰值电流检测为平均电流检测，再次完善了电流模式控制。但是，就象最后一段描述的，必须小心，在 $m=-1/2m_2$，占空比为 1 时，非常容易进入次谐波振荡。

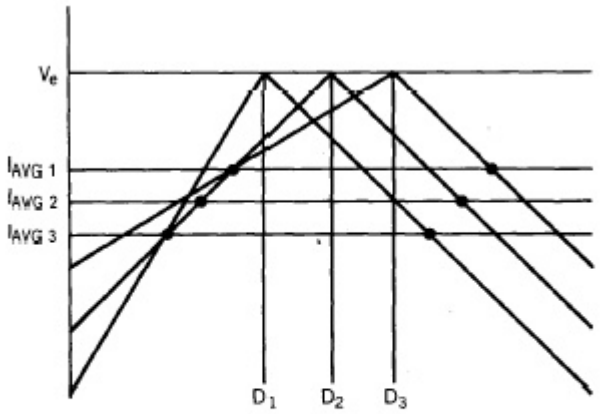

FIGURE 8 - PEAK CURRENT SENSING WITHOUT SLOPE COMPENSATION ALLOWS AVERAGE INDUCTOR CURRENT TO VARY WITH DUTY CYCLE

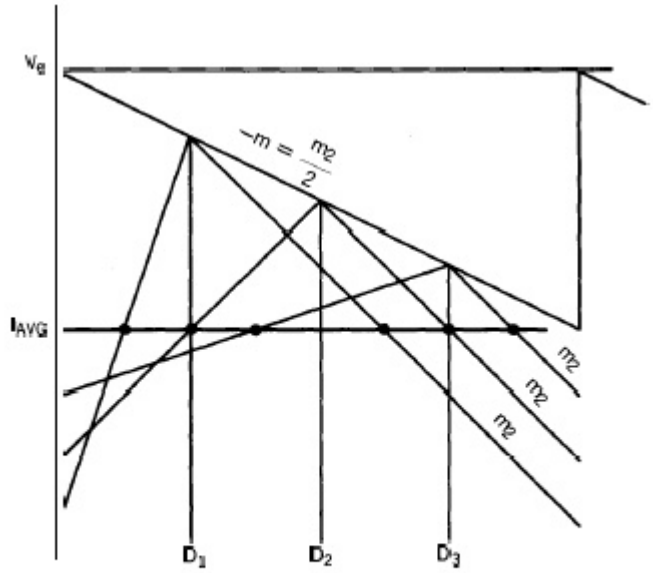

FIGURE 9 - AVERAGE INDUCTOR CURRENT IS INDEPENDENT OF DUN CYCLE AND INPUT VOLTAGE VARIATION FOR A SLOPE COMPENSATION OF m = -½ m_2.

2.5 低纹波电流

从系统的角度来看，低的电感纹波电流是好的，这有很多原因——降低对输出电容的需求、轻载时电流连续、低的输出纹波等等。然而，因为电流检测电路上产生的斜率很小，在很多场合下，小的纹波电流会导致脉宽因随机或同步的噪声而跳动。见图 10。再一次，如果我们对电流波形添加斜坡补偿，将产生一个更稳定的开关点。为了更有利，斜坡补偿的量与电感总电流相比必须是显著的，而不仅仅是纹波电流。通常规定是，斜坡 m 显著地大于 m_2，这时有令人满意的次谐波稳定性。当任何斜坡大于 $m=-1/2m_2$，会使变换器的性能不象一个理想的电流模式变换器，而更象一个电压模式变换器。在电感纹波电流和斜坡补偿间的适当的平衡只能够由基于下一部分中模型导出的等价电路得到。

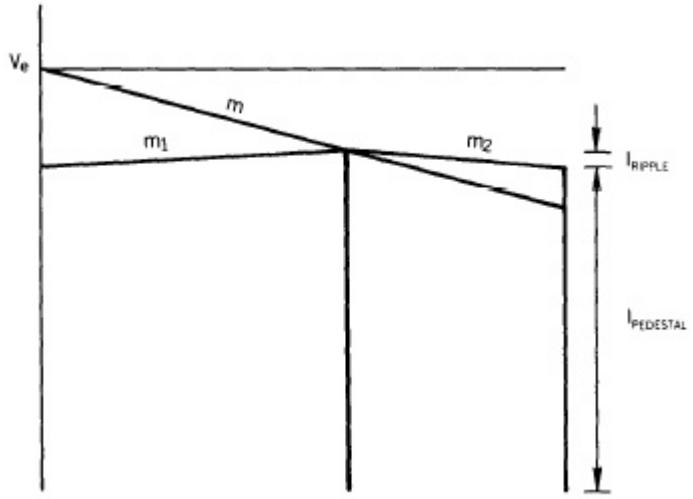

FIGURE 10 - A LARGE PEDESTAL TO RIPPLE CURRENT RATIO.

3.0 小信号交流模型

就象我们已经看到的，电流模式控制方式得的很多缺点可以通过对电流波形添加不同程度的斜坡补偿来减轻或消除。为了评估同样的补偿对闭环响应得全面影响效果，(1) **中运用状态空间平均技术建立了一个** BUCK **调整器得小信号等效电路模型。**

3.1 交流模型的来历

图 11 **显示了一个** BUCK **调整器功率级的等效电路。由此我们可以写出电感电流和电容电压分别于占空比** D **有关得状态空间微分方程。**

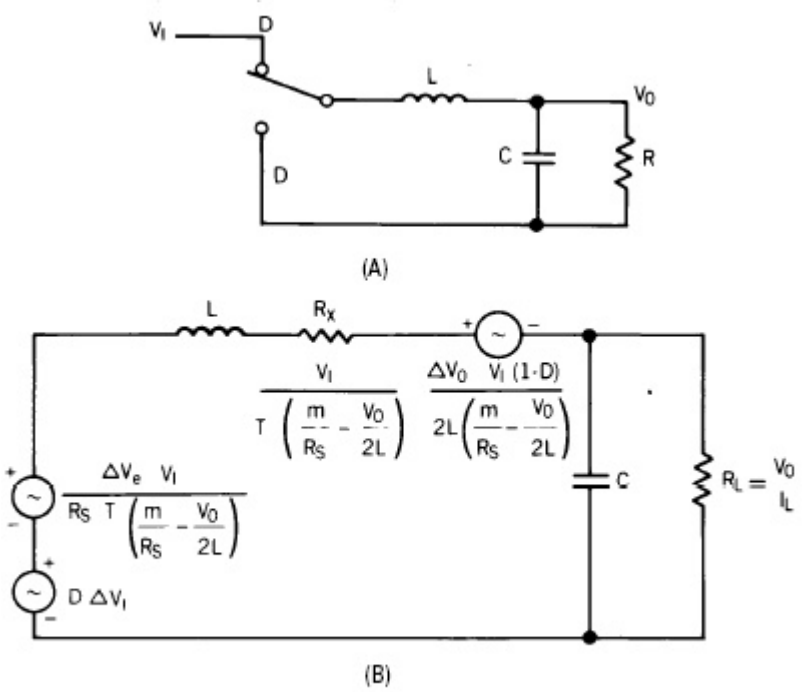

FIGURE 11 BASIC BUCK CONVERTER (A) AND ITS SMALL SIGNAL EQUIVALENT CIRCUIT MODEL (B).

$$\dot{I}_L = \frac{(V_I - V_O)}{L} D - \frac{V_O(1-D)}{L} \qquad (14)$$

$$\dot{V}_O = \frac{I_L}{C} - \frac{V_O}{R} \qquad (15)$$

如果觉得这些等式很烦杂，用 $V_I+\Delta V_I$，$V_O+\Delta V_O$，$D+\Delta D$ 和 $I_L+\Delta I_L$ 代替相应的变量，并忽略 2 阶项，可以生成平均小信号等式。

$$\Delta \dot{I}_L = \frac{D\Delta I_L}{L} - \frac{\Delta V_O}{L} + \frac{V_I \Delta D}{L} \qquad (16)$$

$$\Delta \dot{V}_O = \frac{\Delta I_L}{C} - \frac{\Delta V_O}{CR} \qquad (17)$$

第三个等式，与误差电压 V_e 和占空比相关，可以根据图 6 写为：

$$I_L R_S = V_e - mDT - \frac{(1-D)V_O T R_S}{2L} \qquad (18)$$

对这个等式的扰动象前面给出的那样：

$$\Delta I_L = \frac{\Delta V_e}{R_S} - \Delta DT\left(\frac{m}{R_S} - \frac{V_O}{2L}\right) - \frac{T}{2L}(1-D)\Delta V_O \qquad (19)$$

用式 19 消去式 16、17 中的 ΔD，可以得到状态空间等式：

$$\Delta \dot{I}_L = \frac{D}{L}\Delta V_I + \frac{\Delta V_e V_I}{R_S LT\left(\frac{m}{R_S} - \frac{V_O}{2L}\right)} - \frac{\Delta V_O V_I (1-D)}{2L^2\left(\frac{m}{R_S} - \frac{V_O}{2L}\right)} - \frac{\Delta I_L V_I}{LT\left(\frac{m}{R_S} - \frac{V_O}{2L}\right)} \qquad (20)$$

$$\Delta \dot{V}_O = \frac{\Delta I_L}{C} - \frac{\Delta V_O}{CR} \qquad (21)$$

这些等式的等效电路模型显示在图 11B 中，并在下一部分讨论。

3.2 交流模型讨论

图 11B 的模型可以用来验证和延伸我们先前的观点。理解这个模型的关键是 R_X 和 L 的相互影响相当于斜坡补偿，m 是变化的。在大多数情况下，R_X 和 C 间的影响可忽略。

如果 R_X 比 L 大很多，这样的情况相当于没有或很小的补偿（m=0），变换器将具有一个单极点的响应，是真正的电流模式变换器。如果相对于 L，R_X 很小（$m>>\frac{R_S V_O}{2L}$），就象任何电压模式变换器那样，LRC 输出滤波器产生双极点响应。适当调节 m，可以得到界于这两种极端之间的情况。

特别注意的情况是当 $m=\frac{R_S V_O}{2L}$。由于电感电流的下降斜率（图 6 的 m_2）等于 $\frac{R_S V_O}{L}$，我们能写为 $m=-\frac{1}{2}m_2$。在这一点上，R_X 趋向无穷大，结果是一个理想的电流模式变换器。这个观点和 2.4 部分讨论的一样，即在此点平均电感电流恰好跟随着误差电压。注意，尽管这个补偿对于线性反馈和闭环响应是理想的，当接近由更高的占空比限制的最大误差放大增益时，也许有必要采取更大的斜坡补偿。

推演了等效电路模型，我们将继续它在具体的实例中的应用。图 12 绘制了斜坡补偿对一个典型的 12V 降压 BUCK 调整器在 120Hz 处开环纹波的抑制效果的比较。BUCK 调整电路参数如下：

V_O=12V

V_I=25V

L=200uH

C=300uF

R_S=0.5Ω

R_L=1Ω~12Ω

同样可见，当斜坡补偿接近 $-\frac{1}{2}m_2$，理论上对纹波的抑制趋向无穷大。引入更大的 m 值，纹波抑制的效果降低了，渐渐向电压模式变换器退化。(在这个例子里是-6.4dB)

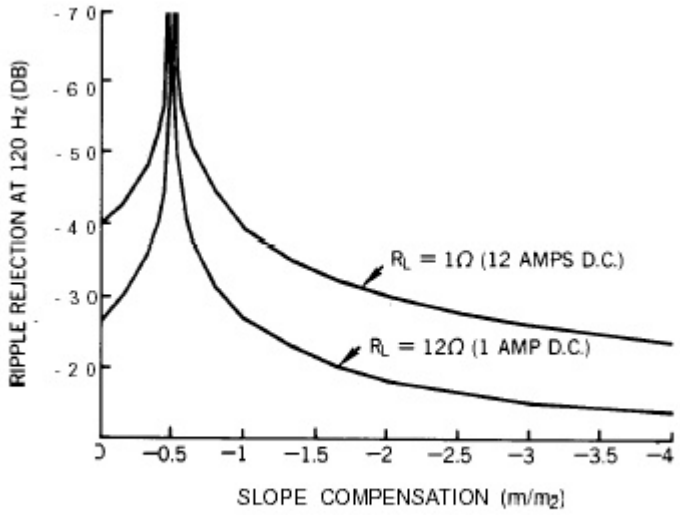

FIGURE 12 - RIPPLE REJECTION AT 120Hz V.S. SLOPE COMPENSATION FOR 1AMP AND 12AMP LOADS.

如果纹波电流与直流电流相比较小，相当于例子中 R_L=1 欧姆的情形。通过保持高的纹波注入比例，可以相应注入更大数值的斜坡补偿。换句话说，要得到给定的纹波注入的比例，所允许的斜坡补偿的变化是与直流电流而不是纹波电流成正比例的。当尝试将低纹波变换器的噪音跳动最小化时，这是一个非常重要的思想。

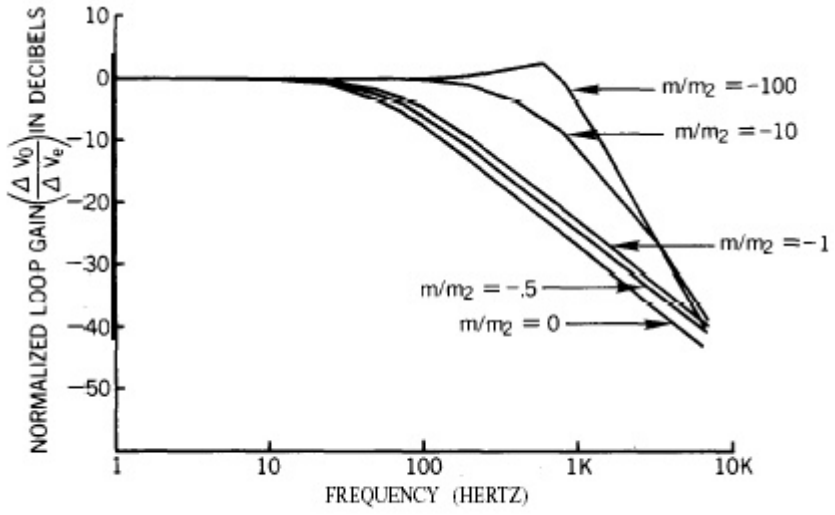

FIGURE 13 - NORMALIZED LOOP GAIN V.S. FREQUENCY FOR VARIOUS SLOPE COMPENSATION RATIO'S.

图 13 显示了图 12 中相同的例子的小信号的频率闭环响应（$\Delta V_O/\Delta V_e$）。在低频下，所有的增益被归一化处理为 0dB，反映了真实情况下不同斜坡补偿 m 变化频率响应的差异。在 $m = -\frac{1}{2}m_2$ 时，产生一个理想的单极点 6dB/频程的延伸。采用更高的比例，响应会接近一个双极点的 12dB/频程的延伸，同时有 180 度的相移。

4.0 控制 IC UC1846 的斜坡补偿

随着集成控制芯片 UC1846 **的引入，实现一个实用的低成本电流模式变换器，最近变的简单了。这个** IC **具备了设计一个固定频率电流模式变换器的需要的所有控制和支持电路。图** 14A **和** B **演示了使用** UC1846 **实现斜坡补偿的两种可选的方法。**

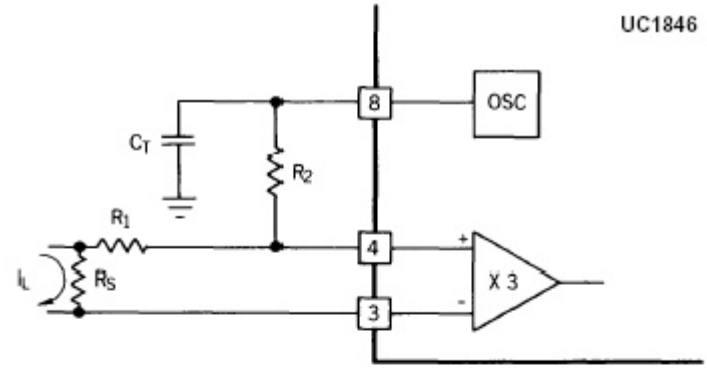

(a) SUMMING OF SLOPE COMPENSATION DIRECTLY WITH SENSED CURRENT SIGNAL

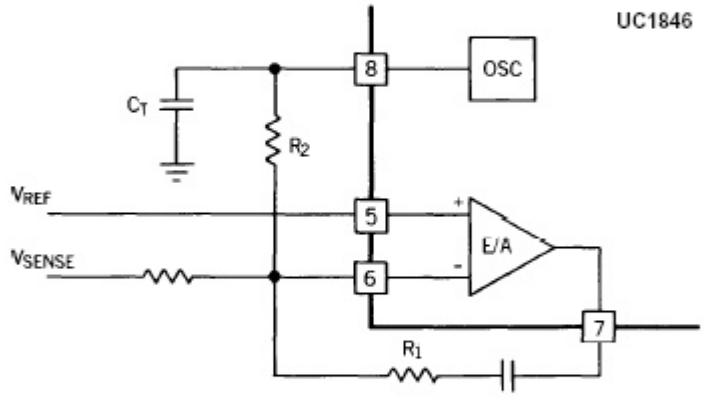

(b) SUMMING OF SLOPE COMPENSATION WITH ERROR SIGNAL

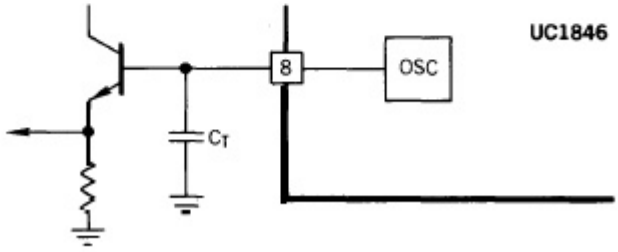

(c) EMITTER FOLLOWER USED TO LOWER OUTPUT IMPEDANCE OF OSCILLATOR.

FIGURE 14 - ALTERNATIVE METHODS OF IMPLEMENTING SLOPE COMPENSATION WITH THE UC1846 CURRENT-MODE CONTROLLER.

直接将补偿和电流采样加在第 4 **脚很容易实现。然而，这样对限流电路带来了一个问题。可替代的方法是引入补偿至误差放大器的反相输入端。这将发挥作用如果（**a**）误差放大器的增益在开关频率处是恒定的常数（这个例子中是** R_1/R_2**），（**b**）当计算所需要的斜坡补偿时，误差放大器和电流放大器的增益都要考虑到。在两种情况下，一旦** R_2 **数值计算出来了，负载对** C_T **的影响就确定了。如果有必要，可以如图** 14C **那样增加一级缓冲级。**

MODELLING, ANALYSIS AND COMPENSATION OF THE CURRENT-MODE CONVERTER

Abstract

As current-mode conversion increases in popularity, several peculiarities associated with fixed-frequency, peak-current detecting schemes have surfaced These include instability above 50% duty cycle, a tendency towards subharmonic oscillation, non-ideal loop response, and an increased sensitivity to noise. This paper will attempt to show that the performance of any current-mode converter can be improved and at the same time all of the above problems reduced or eliminated by adding a fixed amount of "slope compensation" to the sensed current waveform.

1.0 INTRODUCTION

The recent introduction of integrated control circuits designed specifically for current mode control has led to a dramatic upswing in the application of this technique to new designs. Although the advantages of current-mode control over conventional voltage-mode control has been amply demonstrated[1-5], there still exist several drawbacks to a fixed frequency peak-sensing current mode converter. They are (1) open loop instability above 50% duty cycle, (2) less than ideal loop response caused by peak instead of average inductor current sensing, (3) tendency towards subharmonic oscillation, and (4) noise sensitivity, particularly when inductor ripple current is small. Although the benefits of current mode control will, in most cases, far out-weight these drawbacks, a simple solution does appear to be available. It has been shown by a number of authors that adding slope compensation to the current waveform (Figure 1) will stabilize a system above 50% duty cycle. If one is to look further, it becomes apparent that this same compensation technique can be used to minimize many of the drawbacks stated above. In fact, it will be shown that any practical converter will nearly always perform better with some slope compensation added to the current waveform.

The simplicity of adding slope compensation - usually a single resistor - adds to its attractiveness. However, this introduces a new problem - that of analyzing and predicting converter performance. Small signal AC models for both current and voltage-mode PWM's have been extensively developed in the literature. However, the slope compensated or "dual control" converter possesses properties of both with an equivalent circuit different from yet containing elements of each. Although this has been addressed in part by several authors[1,2], there still exists a need for a simple circuit model that can provide both qualitative and quantitative results for the power supply designer.

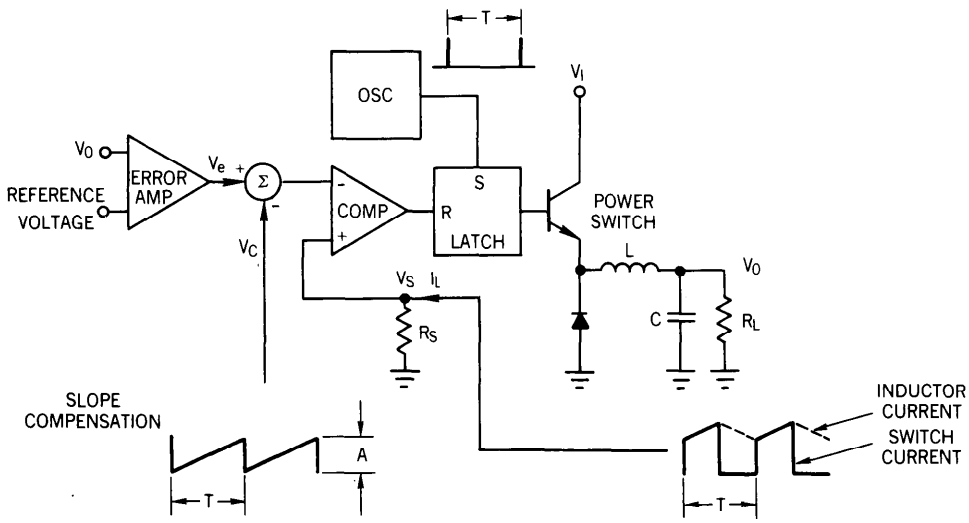

FIGURE 1 - A CURRENT-MODE CONTROLLED BUCK REGULATOR WITH SLOPE COMPENSATION.

The first objective of this paper is to familiarize the reader with the peculiarities of a peak-current control converter and at the same time demonstrate the ability of slope compensation to reduce or eliminate many problem areas. This is done in section 2. Second, in section 3, a circuit model for a slope compensated buck converter in continuous conduction will be developed using the state-space averaging technique outlined in (1). This will provide the analytical basis for section 4 where the practical implementation of slope compensation is discussed.

2.1 OPEN LOOP INSTABILITY

An unconditional instability of the inner current loop exists for any fixed frequency current-mode converter operating above 50% duty cycle - regardless of the state of the voltage feedback loop. While some topologies (most notably two transistor forward converters) cannot operate above 50% duty cycle, many others would suffer serious input limitations if greater duty cycle could not be achieved. By injecting a small amount of slope compensation into the inner loop, stability will result for all values of duty cycle. Following is a brief review of this technique.

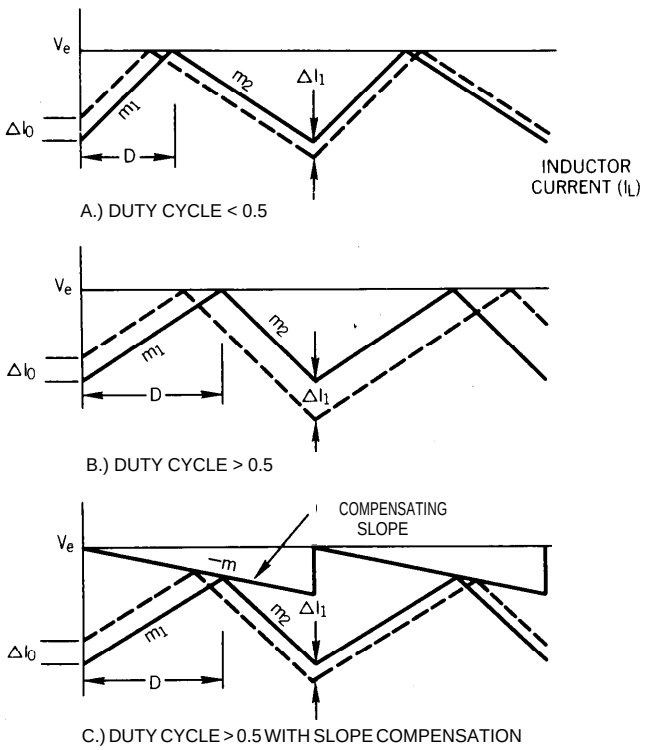

FIGURE 2 - DEMONSTRATION OF OPEN LOOP INSTABILITY IN A CURRENT-MODE CONVERTER.

Figure 2 depicts the inductor current waveform, I_L, of a current-mode converter being controlled by an error voltage V_e. By perturbing the current I_L by an amount ΔI, it may be seen graphically that ΔI will decrease with time for D < 0.5 (Figure 2A), and increase with time for D > 0.5 (Figure 2B). Mathematically this can be stated as

$$\Delta I_1 = -\Delta I_0 \left(\frac{m_2}{m_1}\right) \qquad (1)$$

Carrying this a step further, we can introduce a linear ramp of slope -m as shown in Figure 2C. Note that this slope may either be added to the current waveform, or subtracted from the error voltage. This then gives

$$\Delta I_1 = -\Delta I_0 \left(\frac{m_2 + m}{m_1 + m}\right) \qquad (2)$$

Solving for m at 100% duty cycle gives

$$m > -\tfrac{1}{2} m_2 \qquad (3)$$

Therefore, to guarantee current loop stability, the slope of the compensation ramp must be greater than one-half of the down slope of the current waveform. For the buck regulator of Figure 1, m_2 is a constant equal to $\frac{V_0}{L} R_S$, therefore, the amplitude A of the compensating waveform should be chosen such that

$$A > T R_S \frac{V_0}{L} \qquad (4)$$

to guarantee stability above 50% duty cycle.

2.2 RINGING INDUCTOR CURRENT

Looking closer at the inductor current waveform reveals two additional phenomenon related to the previous instability. If we generalize equation 2 and plot I_n vs nT for all n as in Figure 3, we observe a damped sinusoidal response at one-half the switching frequency, similar to that of an RLC circuit. This ring-out is undesirable in that it (a) produces a ringing response of the inductor current to line and load transients, and (b) peaks the control loop gain at ½ the switching frequency, producing a marked tendency towards instability.

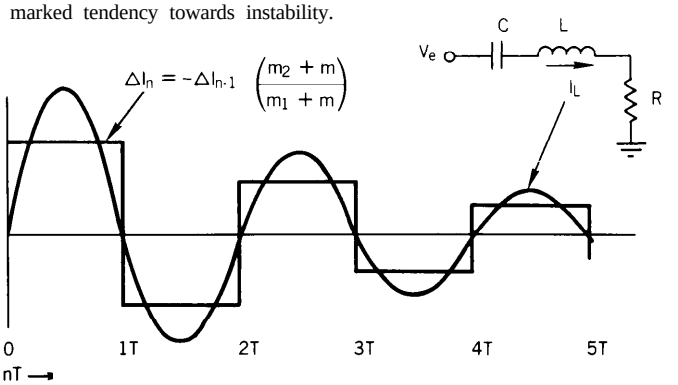

FIGURE 3 - ANALOGY OF THE INDUCTOR CURRENT RESPONSE TO THAT OF AN RLC CIRCUIT.

It has been shown in (1), and is easily verified from equation 2, that by choosing the slope compensation m to be equal to $-m_2$ (the down slope of the inductor current), the best possible transient response is obtained. This is analogous to critically damping the RLC circuit, allowing the current to correct itself in exactly one cycle. Figure 4 graphically demonstrates this point. Note that while this may optimize inductor current ringing, it has little bearing on the transient response of the voltage control loop itself.

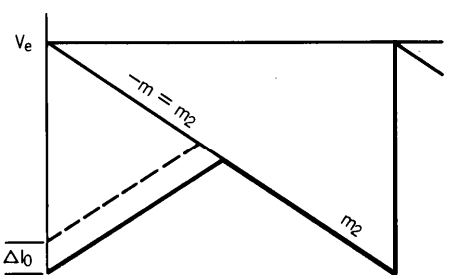

FIGURE 4 - FOR THE CASE OF m = - m_2, A CURRENT PERTURBATION WILL DAMP OUT IN EXACTLY ONE CYCLE.

2.3 SUBHARMONIC OSCILLATION

Gain peaking by the inner current loop can be one of the most significant problems associated with current-mode controllers. This peaking occurs at one-half the switching frequency, and - because of excess phase shift in the modulator - can cause the voltage feedback loop to break into oscillation at one-half the switching frequency. This instability, sometimes called subharmonic oscillation, is easily detected as duty cycle asymmetry between consecutive drive pulses in the power stage. Figure 5 shows the inductor current of a current-mode controller in subharmonic oscillation (dotted waveforms with period 2T).

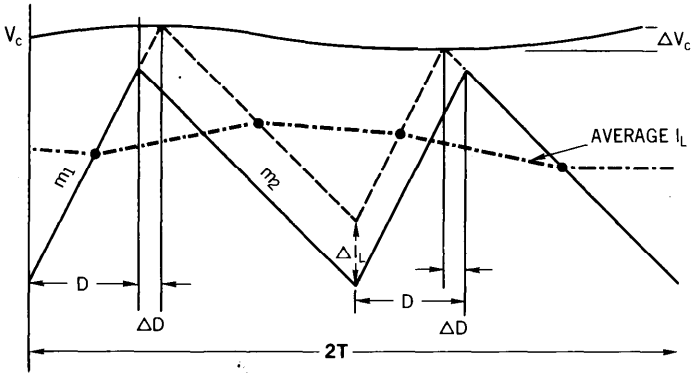

FIGURE 5- CURRENT WAVE FORM (DOTTED) OF A CURRENT-MODE CONVERTER IN SUBHARMONIC OSCILLATION.

To determine the bounds of stability, it is first necessary to develop an expression for the gain of the inner loop at one-half the switching frequency. The technique used in (2) will be paralleled for a buck converter with the addition of terms to include slope compensation

2.3.1 LOOP GAIN CALCULATION AT ½f_s

Referring to figures 5 and 6, we want to relate the input stimulus, ΔV_e, to an output current, ΔI_L. From figure 5, two equations may be written

$$\Delta I_L = \Delta D\, m_1\, T - \Delta D\, m_2\, T \quad (4)$$

$$\Delta V_C = \Delta D\, m_1\, T + \Delta D\, m_2\, T \quad (5)$$

Adding slope compensation as in figure 6 gives another equation

$$\Delta V_e = \Delta V_C + 2\Delta D\, m\, T \quad (6)$$

Using (5) to eliminate ΔV_C from (6) and solving for $\Delta I_L/\Delta V_e$ yields

$$\frac{\Delta I_L}{\Delta V_e} = \frac{m_1 - m_2}{m_1 + m_2 + m} \quad (7)$$

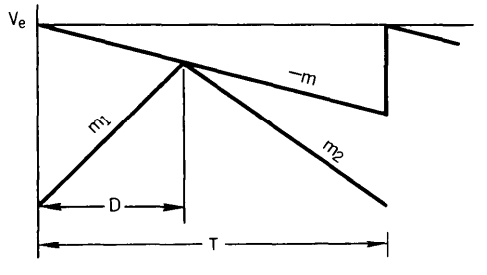

FIGURE 6- ADDITION OF SLOPE COMPENSATION TO THE CONTROL SIGNAL

For steady state condition we can write

$$D\, m_1\, T = (1 - D)\, m_2\, T \quad (8)$$

or

$$D = \frac{-m_2}{m_1 - m_2} \quad (9)$$

By using (9) to reduce (7), we obtain

$$\frac{\Delta I_L}{\Delta V_e} = \frac{1}{1 - 2D\,(1 + m/m_2)} \quad (10)$$

Now by recognizing that ΔI_L is simply a square wave of period 2T, we can relate the first harmonic amplitude to ΔI_L by the factor $4/\pi$ and write the small signal gain at f = ½f_S as

$$\frac{i_L}{v_e} = \frac{4\pi}{1 - 2D\,(1 + m/m_2)} \quad (11)$$

If we assume a capacitive load of C at the output and an error amplifier gain of A, then finally, the expression for loop gain at f = ½f_S is

$$\text{Loop gain} = \frac{\frac{4TA}{\pi^2 C}}{1 - 2D\,(1 + m/m_2)} \quad (12)$$

2.3.2 USING SLOPE COMPENSATION TO ELIMINATE SUBHARMONIC OSCILLATION

From equation 12, we can write an expression for maximum error amplifier gain at f = ½f_S to guarantee stability as

$$A_{max} = \frac{1 - 2D\,(1 + m/m_2)}{\frac{4T}{\pi^2 C}} \quad (13)$$

This equation clearly shows that the maximum allowable error amplifier gain, A_{max}, is a function of both duty cycle and slope compensation A normalized plot of A_{max} versus duty cycle for several values of slope compensation is shown in figure 7. Assuming the amplifier gain cannot be reduced to zero at f = ½f_S, then for the case of m = 0 (no compensation) we see the same instability previously discussed at 50% duty cycle. As the compensation is increased to m = −½m_2, the point of instability moves out to a duty cycle of 1.0, however in any practical

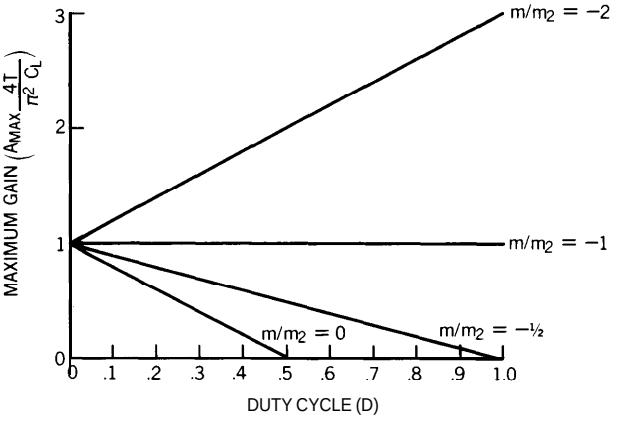

FIGURE 7 - MAXIMUM ERROR AMPLIFIER GAIN AT ½ f_s (NORMALIZED) V.S. DUTY CYCLE FOR VARYING AMOUNTS OF SLOPE COMPENSATION. REFER TO EQUATION 13.

system, the finite value of A_{max} will drive the feedback loop into subharmonic oscillation well before full duty cycle is reached. If we continue to increase m, we reach a point, $m = -m_2$, where the maximum. gain becomes independent of duty cycle. This is the point of critical damping as discussed earlier, and increasing m above this value will do little to improve stability for a regulator operating over the full duty cycle range.

2.4 PEAK CURRENT SENSING VERSUS AVERAGE CURRENT SENSING

True current-mode conversion, by definition, should force the average inductor current to follow an error voltage - in effect replacing the inductor with a current source and reducing the order of the system by one. As shown in Figure 8, however, peak current detecting schemes are generally used which allow the average inductor current to vary with duty cycle while producing less than perfect input to output - or feedforward characteristics. If we choose to add slope compensation equal to $m = -½\ m_2$ as shown in Figure 9, we can convert a peak current detecting scheme into an average current detector, again allowing for perfect current mode control. As mentioned in the last section, however, one must be careful of subharmonic oscillations as a duty cycle of 1 is approached when using $m = -½\ m_2$.

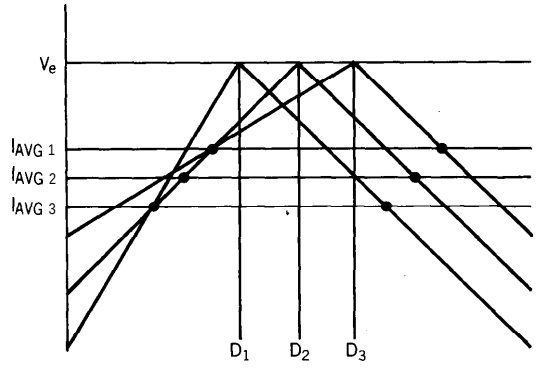

FIGURE 8 - PEAK CURRENT SENSING WITHOUT SLOPE COMPENSATION ALLOWS AVERAGE INDUCTOR CURRENT TO VARY WITH DUTY CYCLE

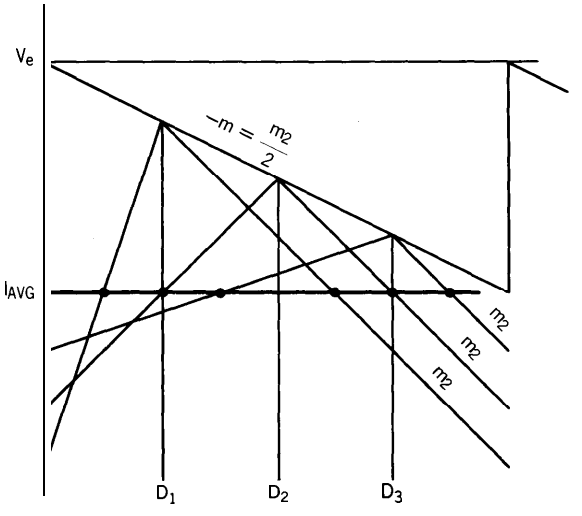

FIGURE 9 - AVERAGE INDUCTOR CURRENT IS INDEPENDENT OF DUN CYCLE AND INPUT VOLTAGE VARIATION FOR A SLOPE COMPENSATION OF $m = -½\ m_2$.

2.5 SMALL RIPPLE CURRENT

From a systems standpoint, small inductor ripple currents are desirable for a number of reasons - reduced output capacitor requirements, continuous current operation with light loads, less output ripple, etc. However, because of the shallow slope presented to the current sense circuit, a small ripple current can, in many cases, lead to pulse width jitter caused by both random and synchronous noise (Figure 10). Again, if we add slope compensation to the current waveform, a more stable switchpoint will be generated. To be of benefit, the amount of slope added needs to be significant compared to the total inductor current - not just the ripple current This usually dictates that the slope m be considerably greater than m_2 and while this is desirable for subharmonic stability, any slope greater than $m = -½\ m_2$ will cause the converter to behave less like an ideal current mode converter and more like a voltage mode converter. A proper trade-off between inductor ripple current and slope compensation can only be made based on the equivalent circuit model derived in the next section.

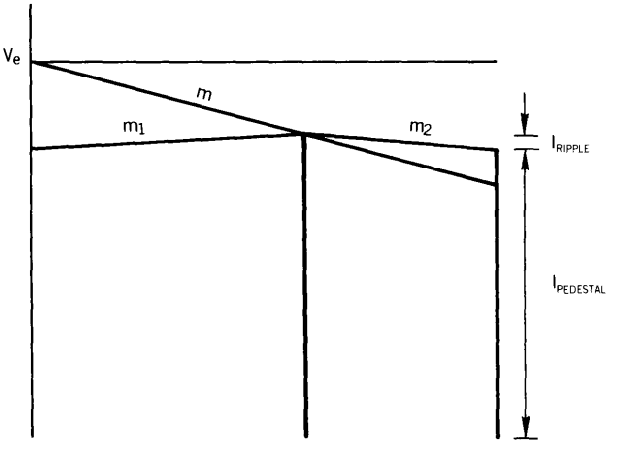

FIGURE 10 - A LARGE PEDESTAL TO RIPPLE CURRENT RATIO.

3.0 SMALL SIGNAL A.C. MODEL

As we have seen, many drawbacks associated with current-mode control can be reduced or eliminated by adding slope compensation in varying degrees to the current waveform. In an attempt to determine the full effects of this same compensation on the closed loop response, a small signal equivalent circuit model for a buck regulator will now be developed using the state-space averaging technique developed in (1).

3.1 A.C. MODEL DERIVATION

Figure 11 a shows an equivalent circuit for a buck regulator power stage. From this we can write two state-space averaged differential equations corresponding to the inductor current and capacitor voltage as functions of duty cycle D

$$\dot{I}_L = \frac{(V_I - V_0)}{L} D - \frac{V_0 (1 - D)}{L} \qquad (14)$$

$$\dot{V}_0 = \frac{I_L}{C} - \frac{V_0}{R} \qquad (15)$$

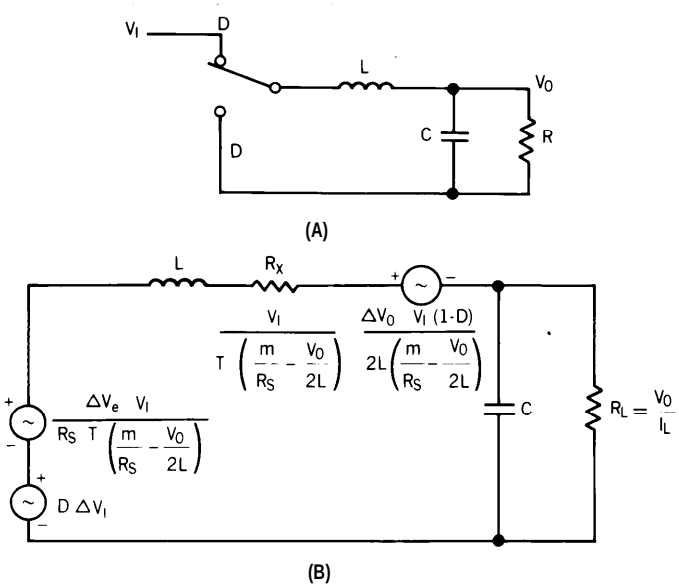

FIGURE 11: BASIC BUCK CONVERTER (A) AND ITS SMALL SIGNAL EQUIVALENT CIRCUIT MODEL (B).

If we now perturb these equations - that in substitute $V_I + \Delta V_I, V_0 + \Delta V_0, D + \Delta D$ and $I_L + \Delta I_L$ for their respective variables - and ignore second order terms, we obtain the small signal averaged equations

$$\Delta \dot{I}_L = \frac{D\Delta I_L}{L} - \frac{\Delta V_0}{L} + \frac{V_I \Delta D}{L} \qquad (16)$$

$$\Delta \dot{V}_0 = \frac{\Delta I_L}{C} - \frac{\Delta V_0}{CR} \qquad (17)$$

A third equation - the control equation - relating error voltage, V_e, to duty cycle may be written from Figure 6 as

$$I_L R_S = V_e - mDT - \frac{(1-D)\, V_0\, T\, R_S}{2L} \qquad (18)$$

Perturbing this equation as before gives

$$\Delta I_L = \frac{\Delta V_e}{R_S} - \Delta D T \left(\frac{m}{R_S} - \frac{V_0}{2L}\right) - \frac{T}{2L}(1-D)\Delta V_0 \qquad (19)$$

By using 19 to eliminate ΔD from 16 and 17 we arrive at the state space equations

$$\Delta \dot{I}_L = \frac{D}{L}\Delta V_I + \frac{\Delta V_e\, V_I}{R_S\, LT\left(\frac{m}{R_S} - \frac{V_0}{2L}\right)} - \frac{\Delta V_0\, V_I\,(1-D)}{2L^2\left(\frac{m}{R_S} - \frac{V_0}{2L}\right)} - \frac{\Delta I_L V_I}{LT\left(\frac{m}{R_S} - \frac{V_0}{2L}\right)} \qquad (20)$$

$$\Delta \dot{V}_0 = \frac{\Delta I_L}{C} - \frac{\Delta V_0}{CR} \qquad (21)$$

An equivalent circuit model for these equations is shown in Figure 11B and discussed in the next section.

3.2 A.C. MODEL DISCUSSION

The model of Figure 11B can be used to verify and expand upon our previous observations. Key to understanding this model is the interaction between R_X and L as the slope compensation, m is changed In most cases, the dependent source between R_X and C can be ignored

If R_X is much greater than L, as is the case for little or no compensation (m = 0), the converter will have a single pole response and act as a true current mode converter. If R_X is small compared to L $\left(m \gg \frac{R_S V_0}{2L}\right)$, then a double pole response will be formed by the LRC output filter similar to any voltage-mode converter. By appropriately adjusting m, any condition between these two extremes can be generated.

Of particular interest is the case when $m = \frac{R_S V_0}{2L}$. Since the down slope of the inductor current (m_2 from Figure 6) is equal to $\frac{R_S V_0}{L}$, we can write $m = -\frac{1}{2}m_2$. At this point, R_X goes to infinity, resulting in an ideal current mode converter. This is the same point, discussed in section 2.4, where the average inductor current exactly follows the error voltage. Note that although this compensation is ideal for line rejection and loop response, maximum error amp gain limitations as higher duty cycles are approached (section 2.3) may necessitate using more compensation.

Having derived an equivalent circuit model, we may now proceed in its application to more specific design examples. Figure 12 plots open loop ripple rejection ($\Delta V_0/\Delta V_I$) at 120Hz versus slope compensation for a typical 12 volt buck regulator operating under the following conditions:

V_0 = 12V
V_I = 25V
L = 200 µH
C = 300µf
T = 20µS
R_S = .5Ω
RL = 1Ω, 12Ω

Again, as the slope compensation approaches $-\frac{1}{2}m_2$, the theoretical ripple rejection is seen to become infinite. As larger values of m are introduced ripple rejection slowly degrades to that of a voltage-mode converter (-6.4dB for this example).

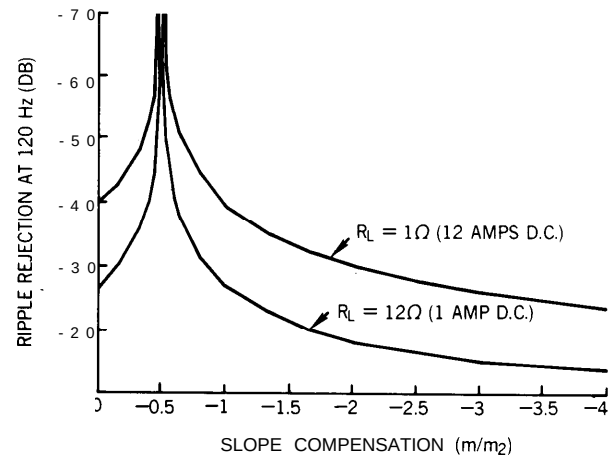

FIGURE 12 - RIPPLE REJECTION AT 120Hz V.S. SLOPE COMPENSATION FOR 1AMP AND 12AMP LOADS.

If a small ripple to D.C. current ratio is used. as is the case for R_L = 1 ohm in the example, proportionally larger values of slope compensation may be injected while still maintaining a high ripple rejection ratio. In other words, to obtain a given ripple rejection ratio, the allowable slope compensation varies proportionally to the average D.C. current, not the ripple current. This is an important concept when attempting to minimize noise jitter on a low ripple converter.

Figure 13 shows the small signal loop response ($\Delta V_0/\Delta V_e$) versus frequency for the same example of Figure 12. The gains have all been normalized to zero dB at low frequency to reflect the actual difference in frequency response as slope compensation m is varied. At m = $-\frac{1}{2}m_2$, an ideal single-pole roll-off at 6dB/octave is obtained. As higher ratios are used. the response approaches that of a double-pole with a 12dB/octave roll-off and associated 180° phase shift

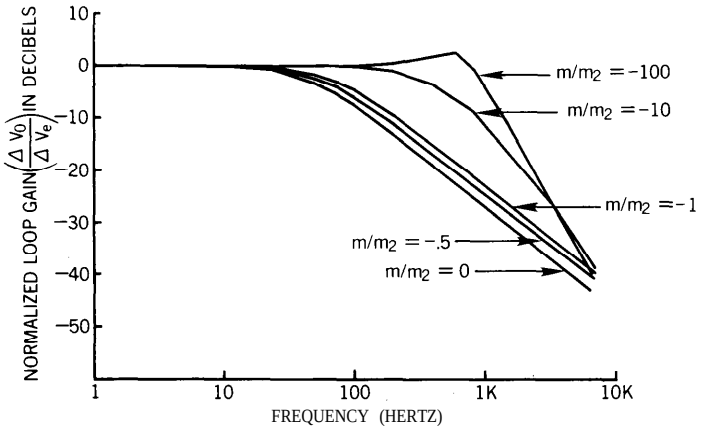

FIGURE 13 - NORMALIZED LOOP GAIN V.S. FREQUENCY FOR VARIOUS SLOPE COMPENSATION RATIO'S.

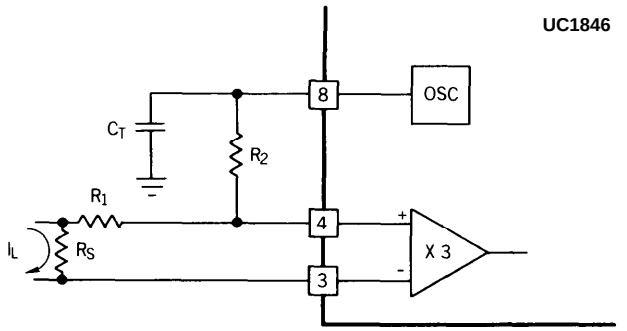

(a) SUMMING OF SLOPE COMPENSATION DIRECTLY WITH SENSED CURRENT SIGNAL

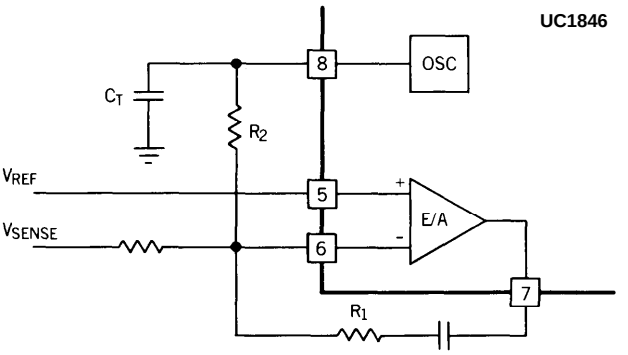

(b) SUMMING OF SLOPE COMPENSATION WITH ERROR SIGNAL

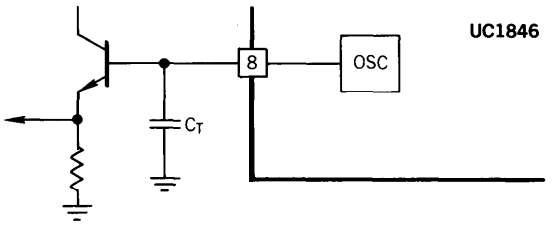

(c) EMITTER FOLLOWER USED TO LOWER OUTPUT IMPEDANCE OF OSCILLATOR.

FIGURE 14 - ALTERNATIVE METHODS OF IMPLEMENTING SLOPE COMPENSATION WITH THE UC1846 CURRENT-MODE CONTROLLER.

4.0 SLOPE COMPENSATING THE UC1846 CONTROL I.C.

Implementing a practical, cost effective current-mode converter has recently been simplified with the introduction of the UC1846 integrated control chip. This I.C. contains all of the control and support circuitry required for the design of a fixed frequency current-mode converter. Figures 14A and B demonstrate two alternative methods of implementing slope compensation using the UC1846. Direct summing of the compensation and current sense signal at Pin 4 is easily accomplished, however, this introduces an error in the current limit sense circuitry. The alternative method is to introduce the compensation into the negative input terminal of the error amplifier. This will only work if (a) the gain of the error amplifier is fixed and constant at the switching frequency (R_1/R_2 for this case) and (b) both error amplifier and current amplifier gains are taken into consideration when calculating the required slope compensation. In either case, once the value of R_2 has been calculated, the loading effect on C_T can be determined and, if necessary, a buffer stage added as in Figure 14C.

REFERENCES

(1) Shi-Ping Hsu, A. Brown, L. Rensink, R. Middlebrook "Modelling and Analysis of Switching DC-to-DC Converters in Constant-Frequency Current-Programmed Mode," PESC '79 Record (IEEE Publication 79CH1461-3 AES), pp. 284-301.

(2) E. Pivit, J. Saxarra, "On Dual Control Pulse Width Modulators for Stable Operation of Switched Mode Power Supplies", Wiss. Ber. AEG-Telefunken 52 (1979) 5, pp. 243-249.

(3) R. Redl, I. Novak "Instabilities in Current-Mode Controlled Switching Voltage Regulators," PESC '81 Record (IEEE Publication 81CH1652-7 AES), pp. 17-28.

(4) W. Bums, A. Ohri, "Improving Off-Line Converter Performance with Current-Mode Control," Powercon 10 Proceedings, Paper B-2, 1983.

(5) B. Holland, "A New Integrated Circuit for Current-Mode Control," Powercon 10 Proceedings, Paper C-2, 1983.

UNITRODE CORPORATION
7 CONTINENTAL BLVD. MERRIMACK, NH 03054
TEL. (603) 424-2410 FAX (603) 424-3460

IMPORTANT NOTICE

Texas Instruments and its subsidiaries (TI) reserve the right to make changes to their products or to discontinue any product or service without notice, and advise customers to obtain the latest version of relevant information to verify, before placing orders, that information being relied on is current and complete. All products are sold subject to the terms and conditions of sale supplied at the time of order acknowledgement, including those pertaining to warranty, patent infringement, and limitation of liability.

TI warrants performance of its semiconductor products to the specifications applicable at the time of sale in accordance with TI's standard warranty. Testing and other quality control techniques are utilized to the extent TI deems necessary to support this warranty. Specific testing of all parameters of each device is not necessarily performed, except those mandated by government requirements.

CERTAIN APPLICATIONS USING SEMICONDUCTOR PRODUCTS MAY INVOLVE POTENTIAL RISKS OF DEATH, PERSONAL INJURY, OR SEVERE PROPERTY OR ENVIRONMENTAL DAMAGE ("CRITICAL APPLICATIONS"). TI SEMICONDUCTOR PRODUCTS ARE NOT DESIGNED, AUTHORIZED, OR WARRANTED TO BE SUITABLE FOR USE IN LIFE-SUPPORT DEVICES OR SYSTEMS OR OTHER CRITICAL APPLICATIONS. INCLUSION OF TI PRODUCTS IN SUCH APPLICATIONS IS UNDERSTOOD TO BE FULLY AT THE CUSTOMER'S RISK.

In order to minimize risks associated with the customer's applications, adequate design and operating safeguards must be provided by the customer to minimize inherent or procedural hazards.

TI assumes no liability for applications assistance or customer product design. TI does not warrant or represent that any license, either express or implied, is granted under any patent right, copyright, mask work right, or other intellectual property right of TI covering or relating to any combination, machine, or process in which such semiconductor products or services might be or are used. TI's publication of information regarding any third party's products or services does not constitute TI's approval, warranty or endorsement thereof.